EXTRACTION OF *IN SITU* COSMOGENIC ^{14}C FROM OLIVINE

Jeffrey S Pigati[1,2] • Nathaniel A Lifton[1] • A J Timothy Jull[3] • Jay Quade[1]

ABSTRACT. Chemical pretreatment and extraction techniques have been developed previously to extract *in situ* cosmogenic radiocarbon (*in situ* ^{14}C) from quartz and carbonate. These minerals can be found in most environments on Earth, but are usually absent from mafic terrains. To fill this gap, we conducted numerous experiments aimed at extracting *in situ* ^{14}C from olivine ($(Fe,Mg)_2SiO_4$). We were able to extract a stable and reproducible *in situ* ^{14}C component from olivine using stepped heating and a lithium metaborate ($LiBO_2$) flux, following treatment with dilute HNO_3 over a variety of experimental conditions. However, measured concentrations for samples from the Tabernacle Hill basalt flow (17.3 ± 0.3 ka[4]) in central Utah and the McCarty's basalt flow (3.0 ± 0.2 ka) in western New Mexico were significantly lower than expected based on exposure of olivine in our samples to cosmic rays at each site. The source of the discrepancy is not clear. We speculate that *in situ* ^{14}C atoms may not have been released from Mg-rich crystal lattices (the olivine composition at both sites was ~$Fo_{65}Fa_{35}$). Alternatively, a portion of the ^{14}C atoms released from the olivine grains may have become trapped in synthetic spinel-like minerals that were created in the olivine-flux mixture during the extraction process, or were simply retained in the mixture itself. Regardless, the magnitude of the discrepancy appears to be inversely proportional to the Fe/(Fe+Mg) ratio of the olivine separates. If we apply a simple correction factor based on the chemical composition of the separates, then corrected *in situ* ^{14}C concentrations are similar to theoretical values at both sites. At this time, we do not know if this agreement is fortuitous or real. Future research should include measurement of *in situ* ^{14}C concentrations in olivine from known-age basalt flows with different chemical compositions (i.e. more Fe-rich) to determine if this correction is robust for all olivine-bearing rocks.

INTRODUCTION

Like other *in situ* cosmogenic nuclides (CNs) that are widely used in Quaternary geology, *in situ* cosmogenic radiocarbon ($t_{1/2}$ = 5.73 ka; *in situ* ^{14}C) is produced in the upper few meters of the Earth's crust by the interaction of cosmic rays and target nuclei in rocks and soil. The potential for using *in situ* ^{14}C to determine surface-exposure ages of Holocene landforms, quantify erosion rates in rapidly denuding landscapes, and decipher complex exposure histories when used in conjunction with other CNs is well known (e.g. Lal 1991; Gosse and Phillips 2001; Miller et al. 2006). Before this potential can be realized, however, reliable protocols for extracting *in situ* ^{14}C from various target minerals must be developed.

Chemical pretreatment and extraction techniques have been developed previously to extract *in situ* ^{14}C from quartz and carbonate (Handwerger et al. 1999; Lifton et al. 2001; Yokoyama et al. 2004; Naysmith 2007; Hippe et al. 2009). These minerals can be found in most environments on Earth, but are usually absent from mafic terrains. To fill this gap, we set out to develop chemical pretreatment and extraction protocols to extract *in situ* ^{14}C from olivine ($(Fe,Mg)_2SiO_4$). *In situ* ^{14}C is produced in olivine primarily via high-energy neutron spallation of Si and O and, to a lesser extent, Fe and Mg, and by capture of negative muons. Olivine is often present in basalt; has a relatively simple stoichiometry and a high ionic density, which limits diffusion (Trull et al. 1991); and is the preferred target mineral for *in situ* ^{3}He. *In situ* ^{10}Be, ^{21}Ne, and ^{26}Al have also been measured in olivine (e.g. Marti and Craig 1987; Nishiizumi et al. 1990; Shimaoka et al. 2002; Blard et al. 2008).

To successfully extract *in situ* ^{14}C from olivine or other host minerals, it is necessary to isolate the *in situ* component from contaminant ^{14}C. At Arizona, this is accomplished in quartz using a rigorous pretreatment process with dilute HF/HNO_3 to isolate quartz grains from other minerals (Kohl and

[1]Department of Geosciences, University of Arizona, Tucson, Arizona 85721, USA.
[2]Present address: US Geological Survey, Denver Federal Center, Box 25046, MS-980, Denver, Colorado 80225, USA. Corresponding author. Email: jpigati@usgs.gov.
[3]Arizona-NSF AMS Facility, Physics Department, University of Arizona, Tucson, Arizona 85721, USA.
[4]ka = thousands of calendar years.

Proceedings of the 20th International Radiocarbon Conference, edited by A J T Jull
RADIOCARBON, Vol 52, Nr 2–3, 2010, p 1244–1260

Nishiizumi 1992), and stepped heating in the presence of a fluxing agent to separate contaminant ^{14}C (released at or below 500 °C) from the *in situ* component (released between 500 and 1100 °C) (Lifton et al. 2001). Unfortunately, olivine is not as resistant as quartz to weathering or chemical treatment, which significantly complicates removal of contaminant ^{14}C without affecting the *in situ* component.

In this study, we experimented with different combinations of inorganic acids, varying acid strengths, and treatment duration, in concert with stepped heating, to find a pretreatment that would eliminate contaminant ^{14}C while retaining the *in situ* component. We used 4 criteria to determine the success or failure of a given experiment: (1) identification of contaminant ^{14}C; (2) separation of contaminant ^{14}C and *in situ* ^{14}C; (3) maximization of the *in situ* ^{14}C yield, assuming that the first 2 criteria were met; and (4) complete recovery of *in situ* ^{14}C from samples (i.e. negligible yield of *in situ* ^{14}C during the last heating step). We then applied our pretreatment and extraction protocols from the "successful" experiments to olivine from 2 calibration sites, the Tabernacle Hill basalt flow in central Utah and the McCarty's basalt flow in western New Mexico. Agreement between measured *in situ* ^{14}C concentrations and theoretical concentrations for our samples based on exposure of olivine to cosmic rays at each site would allow the use of *in situ* ^{14}C for cosmogenic research in terrain with olivine-bearing rocks.

CALIBRATION SITES

We selected calibration sites for this study based on the following criteria: (1) volcanic flows that contain at least 5–10% olivine; (2) olivine grains were not visibly altered (e.g. to iddingsite); (3) the ages of the flows are well constrained by independent dating techniques; (4) primary flow features were present and well preserved; and (5) flow surfaces appeared to have been continuously exposed to cosmic rays since the time of eruption (i.e. no evidence of episodic burial or shielding). We identified 2 sites for this study that met each of these criteria: the Tabernacle Hill basalt flow in the Black Rock Desert of south-central Utah and the McCarty's basalt flow in the Zuni-Bandera Volcanic Field in western New Mexico (Table 1, Figure 1).

Table 1 Summary of information for sampling sites.

	Exposed samples					*Shielded sample*
	Tabernacle Hill				McCarty's flow	Miocene flow
Sample ID	TH-1	TH-12	TH-13	TH-15	McC-1b	AZ02-2
Site information						
Latitude (°N)	38.93	38.93	38.93	38.92	34.84	34.83
Longitude (°W)	112.52	112.52	112.53	112.50	107.92	111.61
Elevation (m)	1454	1464	1461	1479	2185	1979
Independent age (^{14}C ka)	14.4 ± 0.1	14.4 ± 0.1	14.4 ± 0.1	14.4 ± 0.1	3.0 ± 0.1	—
Reference[a]	1	1	1	1	2	3
Calibrated age (ka)[b]	17.3 ± 0.4	17.3 ± 0.4	17.3 ± 0.4	17.3 ± 0.4	3.2 ± 0.2	17–21 Ma
Sample information						
Density (g cm^{-3})[c]	2.15 ± 0.20	—	—	—	2.30 ± 0.20	—
Thickness (cm)	2 ± 1	3 ± 1	3 ± 1	4 ± 1	5 ± 1	—
Correction factors[d]						
Sample thickness	1.01 ± 0.01	1.02 ± 0.01	1.02 ± 0.01	1.03 ± 0.01	1.04 ± 0.01	—
Topographic shielding	1.00 ± 0.05	1.00 ± 0.05	1.00 ± 0.05	1.00 ± 0.05	1.00 ± 0.05	—
Chemical composition[e]	—	1.15 ± 0.03	1.16 ± 0.05	1.14 ± 0.03	1.21 ± 0.08	1.17 ± 0.05

[a]Reference: 1 = Oviatt and Nash (1989); 2 = Laughlin et al. (1994); 3 = Kamilli and Richard (1998).

[b]Calibrated ages calculated using IntCal04.14C data set (CALIB 5.1.0.Beta, Stuiver and Reimer 1993; Reimer et al. 2004).

[c]Density of samples TH-12, -13, and -15 are assumed to be the same as TH-1.

[d]Corrections made using protocols of Lifton et al. (2001).

[e]Normalized to a pure SiO_2 composition using fast neutron flux spectrum of Gordon et al. (2004), following Lifton et al. (2001). Chemical composition of TH-1 is assumed to be identical to TH-15.

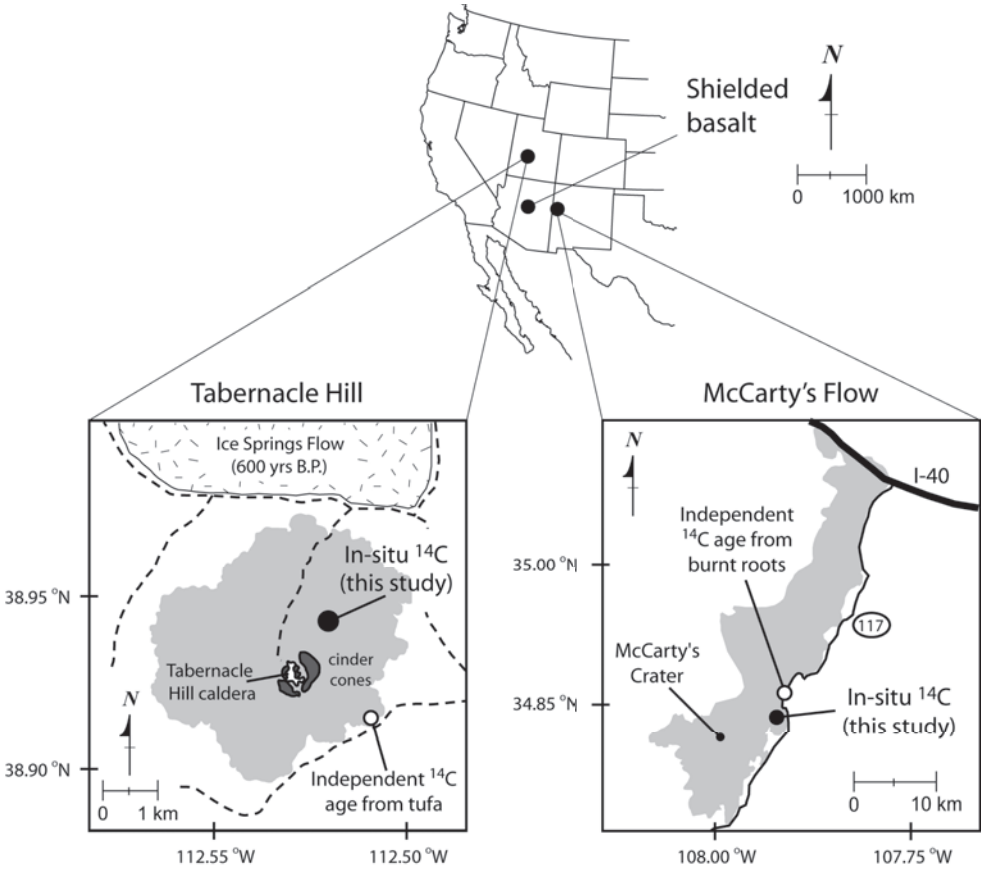

Figure 1 Locations of the Tabernacle Hill basalt flow in the Black Rock Desert of central Utah, the McCarty's basalt flow in the Zuni-Bandera Volcanic Field of western New Mexico, and the shielded basalt sample from northern Arizona. Specific locations (latitude, longitude, elevation) for all samples are provided in Table 1. Locations of independent age control sample sites are denoted by open circles.

The Tabernacle Hill basalt flow (38.93°N, 112.52°W) is a small, essentially circular basalt flow that erupted into pluvial Lake Bonneville when the lake was at or near the Provo shoreline (Oviatt and Nash 1989; Godsey et al. 2005). The age of the flow is constrained by ^{14}C ages of 14.5 ± 0.1 ^{14}C ka, when the lake drained catastrophically from the Bonneville highstand to the Provo level during the Bonneville Flood (Oviatt et al. 1992), and 14.3 ± 0.1 ^{14}C ka, obtained from dense tufa on the outer margin of the flow in association with the Provo-level shoreline (Oviatt and Nash 1989). ^{14}C ages from tufa can be problematic, but we consider the tufa age here to be reliable for 2 reasons. First, while ^{14}C ages obtained from tufa can be younger than the true age if aqueous carbon species are introduced by groundwater (open-system behavior), the dated tufa was collected from beneath an overhanging ledge of basalt. Thus, it has been effectively shielded from percolating groundwater since its formation. Second, ^{14}C ages from tufa can be older than the true age if the carbon isotopic composition of the original host water was not in equilibrium with atmospheric carbon during precipitation of the tufa (carbon reservoir effects). However, carbon reservoir effects in the Bonneville paleolake system were likely <500 yr (Broecker and Kaufman 1965) and probably <200 yr (Benson 1978). We therefore consider the age of 14.3 ± 0.1 ^{14}C ka to be a reliable minimum age for the Tabernacle Hill eruption, and adopt an age of 14.4 ± 0.1 ^{14}C ka (17.3 ± 0.4 ka; ^{14}C age calibrated using

the IntCal04.14C data set (CALIB 5.1.0.Beta, Stuiver and Reimer 1993; Reimer et al. 2004)) as the age of the flow.

Much of the surface of the Tabernacle Hill flow is well preserved and many primary features, including pahoehoe ropes and pressure ridges (tumuli), are present, particularly in a grassy plain north of the caldera (Figure 2a). The excellent preservation of the flow and its well-established age have led to its use as a calibration site for estimating production rates of other *in situ* cosmogenic nuclides, including ^{3}He (Cerling 1990), ^{21}Ne (Poreda and Cerling 1992), and ^{36}Cl (Zreda et al. 1991; Phillips et al. 1996).

Figure 2 Photographs of sampled surfaces. (a) Pahoehoe ropes at the Tabernacle Hill basalt flow (sample TH-13). (b) Glassy surface at the McCarty's basalt flow (sample McC-1b). The areas around these sites were relatively flat and did not show any evidence of mass wasting or past shielding.

The McCarty's basalt flow (34.84°N, 107.92°W) is the youngest flow in the Zuni-Bandera Volcanic Field and is located within the boundaries of the El Malpais National Monument (EMNM). The age of the McCarty's flow is constrained by 2 ^{14}C dates that were obtained from burned tree roots located just below the base of the flow (Laughlin et al. 1994). The ^{14}C ages have a weighted mean age of 3.0 ± 0.1 ^{14}C ka (3.2 ± 0.2 ka), which we adopt as the exposure age of the flow. The surface of this flow is remarkably well preserved. A thin veneer of volcanic glass that originally covered the surface of the flow is still present in many areas (Figure 2b), and primary pahoehoe features are common.

METHODS

Field Methods

We collected samples from the top few centimeters of well-preserved pahoehoe ropes at several locations at each site and measured the inclination to the horizon at 30° azimuthal increments using a hand-held clinometer to determine the degree of topographic shielding. We did not find any evidence of episodic burial by dust or ash at either location. Both the Black Rock Desert and EMNM receive snow during winter months, but annual snowfall is <15 cm yr^{-1} at both locations and lasts only a few months at most, which would not significantly impact the flux of high-energy neutrons or muons responsible for production of *in situ* ^{14}C (Lal 1988).

Laboratory Methods

We first measured the average thickness of all samples, along with representative densities, in order to calculate depth-integrated production rates. Samples were crushed and sieved to isolate the 0.25–0.50 mm and 0.5–1.0 mm size fractions. Olivine was isolated from the matrix material using a Frantz Magnetic Barrier Laboratory Separator (model LB-1) and heavy liquids (lithium metatungstate at a density of 2.93–2.95 g cm^{-3}). Our goal for each sample was to recover at least 20–30 g of olivine so that multiple measurements could be made on the same aliquot to facilitate direct comparison of the results. (A single *in situ* ^{14}C measurement requires up to 5.0 g of the target mineral.) To achieve this, we typically crushed, sieved, and processed 2–3 kg of basalt per sampling location.

We experimented with several combinations of HF, HCl, and HNO_3 under a variety of experimental conditions in an attempt to eliminate contaminant ^{14}C while preserving the *in situ* ^{14}C component (summarized in Table 2). For each experiment, the chemical treatment was performed the day before the extraction, and the grains were stored under low vacuum (~90 kPa) overnight to minimize the amount of time that they were exposed to the atmosphere.

In situ ^{14}C was extracted from the treated olivine grains using the modified *in situ* ^{14}C extraction system at the University of Arizona as described in detail in Pigati et al. (this volume). Briefly, on day 1, a high-purity alumina (Al_2O_3) boat and 20.0 g of lithium metaborate ($LiBO_2$) powder were preheated to 1200 ºC for 1 hr in ~6.7 kPa of ultra-high-purity (UHP) O_2 to remove atmospheric carbon and other contaminants from the fluxing agent and boat prior to introducing the sample. On day 2, the boat was removed from the extraction system, olivine grains were loaded onto the now-solidified $LiBO_2$ surface, and returned to the furnace chamber. For all experiments, the temperature of the furnace was initially raised to 170 °C for 1 hr to remove adsorbed atmospheric gases (mostly water). The furnace chamber was then filled with 6.7 kPa of UHP O_2 and the temperature was raised to the desired set point where sample CO_2 and other condensable gases were collected in a coil trap using liquid nitrogen.

Table 2 Summary of experimental results.[a]

Lab #	AMS #	Sample #	Size (mm)	HNO_3[b]	HCl[b]	HF/HNO_3[b]	Step[c]	^{14}C yield (10^3 atoms g^{-1})[d]
				Tabernacle Hill				
HF experiments								
RN-725	AA-53333	TH-1	0.25–0.50	10%, 1 hr	10%, 1 hr	1%, 2 hr	fine	62 ± 8
RN-728	AA-53333	TH-1	0.25–0.50	10%, 1 hr	10%, 1 hr	1%, 1 hr	fine	104 ± 11
RN-739	AA-55357	TH-13	0.5–1.0	1%, 1 hr	1%, 1 hr	1%, 0.25 hr	fine	344 ± 17
HCl experiments								
RN-721	AA-55357	TH-13	0.5–1.0	0.1%, 1.5 hr	0.1%, 1.5 hr	—	fine	372 ± 18
RN-730	AA-55357	TH-13	0.25–0.50	10%, 1 hr[e]	10%, 1 hr	—	fine	555 ± 24
RN-736	AA-55357	TH-13	0.25–0.50	1%, 1 hr	1%, 1 hr	—	fine	819 ± 39
HNO_3 experiments								
RN-741	AA-55359	TH-15	0.5–1.0	10%, 3 hr	—	—	fine	107 ± 11
RN-745	AA-55359	TH-15	0.5–1.0	10%, 2 hr	—	—	fine	224 ± 12[e]
RN-751	AA-55359	TH-15	0.5–1.0	10%, 1.5 hr	—	—	fine	102 ± 10
RN-754	AA-55359	TH-15	0.5–1.0	10%, 1.5 hr	—	—	coarse	114 ± 9
RN-756	AA-53333	TH-15	0.25–0.50	10%, 1.5 hr	—	—	coarse	123 ± 9
RN-774	AA-55359	TH-15	0.5–1.0	5%, 1.5 hr	—	—	coarse	75 ± 7
RN-776	AA-55359	TH-15	0.5–1.0	1%, 1.5 hr	—	—	coarse	97 ± 8
RN-777	AA-55359	TH-15	0.5–1.0	0.1%, 1.5 hr	—	—	fine	151 ± 9
RN-779	AA-55356	TH-12	0.5–1.0	0.1%, 0.25 hr	—	—	fine	119 ± 9
						Weighted mean (HNO_3 only)		**108 ± 9**
				McCarty's flow				
RN-771	AA-60994	McC-1b	fine	10%, 1.5 hr	—	—	coarse	27 ± 5
RN-772	AA-60994	McC-1b	fine	10%, 1.5 hr	—	—	coarse	32 ± 6
						Weighted mean		**29 ± 4**
				Shielded basalt				
RN-757	AA-58546	AZ02-2	fine	10%, 1.5 hr	—	—	coarse	0 ± 4

[a] All uncertainties are given at the 1-σ level.

[b] Acid concentration (vol. %), Duration of acid treatment. 1% HF/HNO_3 = 1% HF + 1% HNO_3. HNO_3 and HCl treatments were carried out at 70 °C; HF/HNO_3 treatments were done at 95 °C.

[c] Temperature increment (or step) between 600 and 1100 °C. Fine = 600, 700, 900, and 1100 °C; Coarse = 600 and 1100 °C. The duration of each step was 1 hr, except for the 1100 °C step, which was 3 hr.

[d] Concentration of all aliquots collected between 600 and 1100 °C, normalized to a pure SiO_2 composition, CN production at the ground surface, and no topographic shielding (after Lifton et al. 2001).

[e] Concentration is >2 σ from the weighted mean. Not included in the weighted mean calculation.

Fine step-heating experiments were conducted with temperature steps at 300, 500, 600, 700, 900, and 1100 °C. Condensable gases were collected for 1 hr for each temperature step below 1100 °C and after 3 separate 1-hr periods at 1100 °C (a total of 8 aliquots). Coarse step-heating experiments were conducted with steps at 500 and 600 °C for 1 hr each (gases collected during the 500 °C step were discarded) and 1100 °C for 3 hr (a total of 2 aliquots). The collected gases were transferred to a purification system where contaminants, including SO_X, NO_X, and halide species, were removed using a series of passive traps. The volumetric yield was measured and the CO_2 was diluted with ^{14}C-free CO_2 to a total mass of 1–2 mL (0.5–1 mg C equivalent) for subsequent conversion to graphite. CO_2 was converted to graphite on a separate vacuum system via catalytic reduction of CO (after Slota et al. 1987) and submitted to the Arizona Accelerator Mass Spectrometry (AMS) Facility for analysis.

Treatment of Raw Data

The measured concentration of *in situ* ^{14}C atoms in each temperature step was normalized to production at the ground surface and open-sky conditions (i.e. no topographic shielding), and a pure SiO_2

composition. We followed the protocols of Lifton et al. (2001) for each correction, except that we used the fast neutron flux spectrum of Gordon et al. (2004), rather than Nieminen et al. (1985), for the SiO_2 normalization. The magnitude of the corrections for sample thickness were on the order of a few percent for the Tabernacle Hill and McCarty's flow samples, and topographic shielding corrections were negligible at both locations; normalization to a pure SiO_2 composition required corrections of 14–21% (Table 1). Major element analytical results for selected samples are included in Table A1 of the Appendix.

The total *in situ* ^{14}C concentration in each olivine sample was taken as the sum of the yields for all temperature steps above 600 °C, including all 3 hr at 1100 °C. Unlike quartz, we found that the yield at 600 °C for olivine was significant, up to 32% of the total, and is more likely to represent contamination than the *in situ* component. Yields for all temperature steps are included in Table A2 in the Appendix.

Weighted mean values of the *in situ* ^{14}C concentrations for each sample set were calculated using $1/\sigma_i^2$ weighting, where σ_i is the analytical error associated with the individual sample measurement (Bevington and Robinson 1992: Equation 4.17). We calculated both the standard error of the weighted mean (Bevington and Robinson 1992: Equation 4.19; "internal" error) and the weighted average variance of the data (Bevington and Robinson 1992: Equation 4.22; "external" error), and took the larger of the two as the uncertainty associated with the weighted mean, which we report at the 1-σ confidence level. All uncertainties were fully propagated by combining errors in quadrature, neglecting covariance terms.

EXPERIMENTAL RESULTS

We initially conducted 3 step-heating experiments on aliquots of olivine from Tabernacle Hill that were successively treated with dilute HNO_3, HCl, and HF/HNO_3 solutions (in that order) over a period of 3 days. Between each step, the olivine grains were thoroughly rinsed with ASTM Type 1, 18.2 MΩ (hereafter "ultrapure") water and dried overnight in a vacuum oven at 75 °C. The duration of the HNO_3 and HCl treatments was 1 hr in all 3 experiments, and the duration of exposure to the HF/HNO_3 solution ranged between 0.25 and 2 hr (Table 2).

Low concentrations of *in situ* ^{14}C in the 700 ºC step (yields were (0 ± 3) and $(14 \pm 4) \times 10^3$ atoms g^{-1}) show that separation of contaminant and *in situ* ^{14}C was achieved for the extended (1 hr; RN-728 and 2 hr; RN-725) HF/HNO_3 treatments, but not for the brief (0.25 hr; RN-739) treatment (Figure 3a, Table A2). However, the results also show that a significant portion of the *in situ* component was removed by the HF/HNO_3 solution, as the *in situ* ^{14}C yields decreased as the duration of acid treatments increased. This suggests that the HF/HNO_3 solution likely removed both the contaminant and *in situ* components simultaneously. Partial dissolution of the olivine was observed during both of the extended experiments, which supports this interpretation. As a result, the use of the HF/HNO_3 solution was abandoned in favor of a less aggressive treatment.

We conducted 3 step-heating experiments on Tabernacle Hill olivine following treatment with dilute HNO_3 and HCl solutions (in that order) over a period of 2 days. Again, the olivine grains were thoroughly rinsed in ultrapure water, filtered, and dried overnight in a vacuum oven at 75 °C between each step. We varied the concentration of each acid between 0.1 and 10%, and the duration of the acid treatments ranged between 1 and 1.5 hr (Table 2). Significant ^{14}C yields ranging between (141 ± 12) and $(250 \pm 20) \times 10^3$ atoms g^{-1} were obtained for the 700 °C step (Figure 3b, Table A2) in all 3 experiments, which suggests that these combinations of acids, strength, and reaction duration were not sufficient to remove the contaminant ^{14}C.

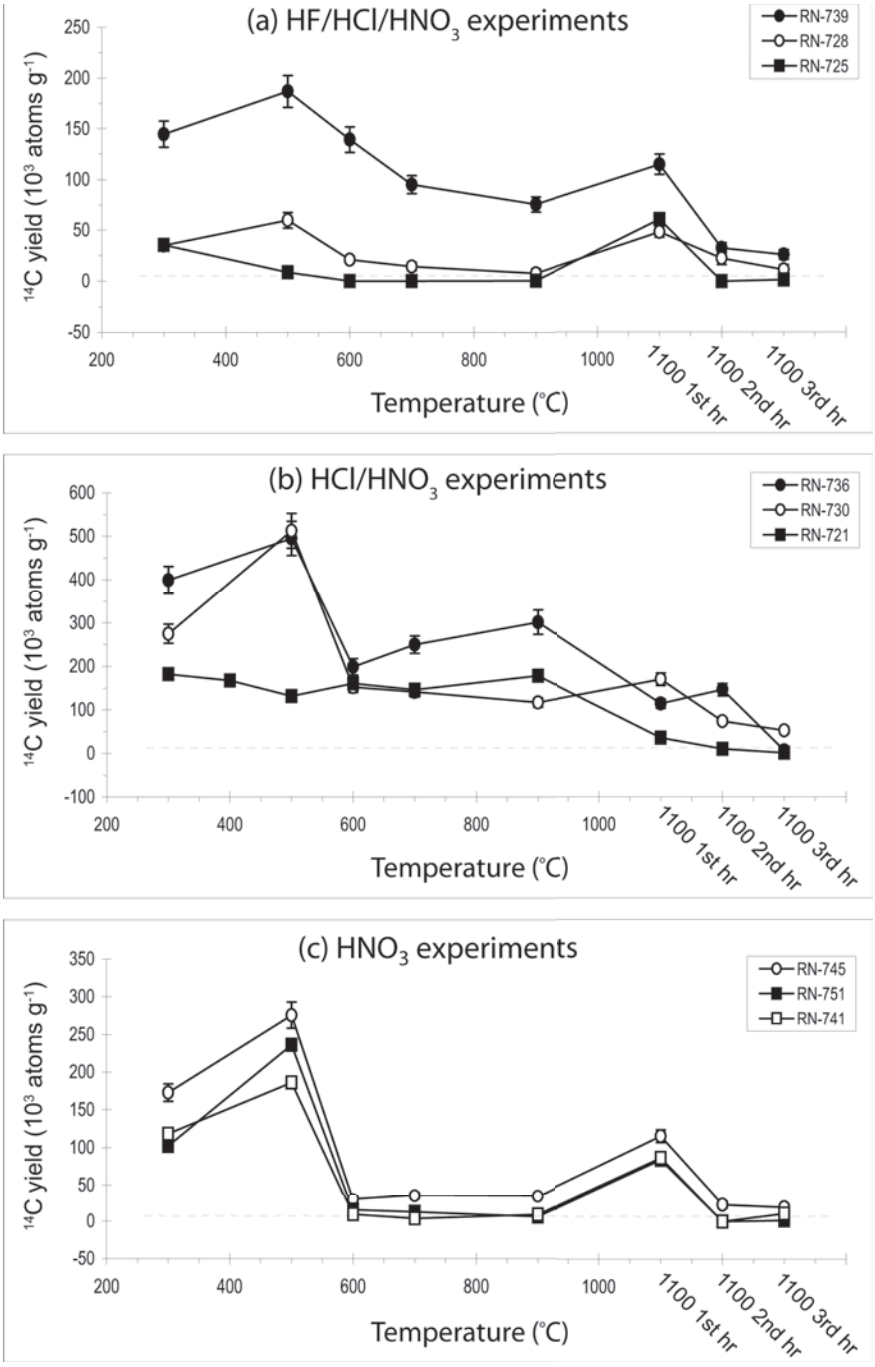

Figure 3 Results of step-heating experiments with (a) HF/HNO_3, HCl, and HNO_3, (b) HCl and HNO_3, and (c) HNO_3 only. The types of acids, acid strengths, duration of exposure to the acid solutions, and step-heating increments are summarized in Table 2. Contaminant ^{14}C is released from olivine at temperatures of 600 °C or below, whereas *in situ* ^{14}C is released above this temperature, predominantly at 1100 °C and above. Significant yields at 700 °C indicate incomplete removal of contaminant ^{14}C (e.g. RN-739, -736, -730, and -721).

We then conducted 3 step-heating experiments on aliquots of the Tabernacle Hill olivine that were treated only with HNO_3. Acid concentrations ranged from 0.1 to 10%, and durations of the treatments ranged from 1.5 to 3 hr (Table 2). As before, olivine grains were thoroughly rinsed in ultrapure water, filtered, and dried overnight in a vacuum oven at 75 °C. The results of these experiments show that the duration and strength of the HNO_3 treatments were sufficient to remove the contaminant ^{14}C for samples RN-741 and RN-751 (yields were (3 ± 3) and (12 ± 3) × 10^3 atoms g^{-1}, respectively, for the 700 °C step for these samples). Moreover, the magnitude of the *in situ* component does not show a clear relationship with the duration of the acid treatment, which suggests that there is a stable *in situ* ^{14}C component in the Tabernacle Hill olivine that was not significantly affected by the HNO_3. *In situ* ^{14}C yields for samples RN-741, RN-745, and RN-751, were (107 ± 11), (224 ± 12), and (102 ± 10) × 10^3 atoms g^{-1}, respectively (Figure 3c; Table 2).

To verify these results, we conducted 6 additional step-heating experiments on the Tabernacle Hill olivine samples. As before, gases evolved at temperatures of 500 °C and below were discarded. We varied the duration of the HNO_3 treatments (0.25 to 1.5 hr), acid strength (0.1 to 10%), and grain size (0.25–0.50 and 0.5–1.0 mm diameter) to optimize the yield while minimizing the contaminant component. The *in situ* ^{14}C yields from these experiments ranged between (75 ± 7) × 10^3 atoms g^{-1} and (151 ± 9) × 10^3 atoms g^{-1}, and do not show a clear relationship with duration of the acid treatments or acid strength. The weighted mean of the HNO_3 experiments, excluding sample RN-745, is (108 ± 9) × 10^3 atoms g^{-1} (n = 8). We exclude the results from this sample for 2 reasons. First, its concentration ((224 ± 12) × 10^3 atoms g^{-1}) falls well outside of the 2-σ confidence interval of the weighted mean calculated from the entire sample population. Second, while the *in situ* ^{14}C yield profile of this sample is nearly identical to the other 2 samples that were treated in the same manner (RN-741 and RN-751; Figure 3c), the ^{14}C yields of each temperature step for sample RN-745 are systematically higher than the other samples by approximately (20 to 25) × 10^3 atoms g^{-1} per step. The source of this offset is unclear.

Aliquots of olivine from the surface of the McCarty's basalt flow in western New Mexico (sample McC-1b) were treated with 10% HNO_3 for 1.5 hr before each extraction. The weighted mean *in situ* ^{14}C yield for 2 aliquots of olivine from the McCarty's flow was (29 ± 4) × 10^3 atoms g^{-1} (n = 2).

Finally, we analyzed samples from a Miocene basalt flow that is exposed by a deep roadcut along Interstate 17, ~40 km south of Flagstaff, Arizona (Kamilli and Richard 1998). The base of the roadcut is shielded by ~20 m of rock and, therefore, the samples should not contain a measurable *in situ* ^{14}C component. We used a sample taken from near the base, #AZ02-2, as a procedural blank to determine whether we introduced ^{14}C during the chemical pretreatment, extraction, purification, or graphitization processes. Following treatment with 10% HNO_3 for 1.5 hr, the *in situ* ^{14}C yield for the shielded olivine was (0 ± 4)× 10^3 atoms g^{-1}, which indicates that we have not introduced more than 4 × 10^3 ^{14}C atoms g^{-1} during the pretreatment, extraction, purification, and graphitization processes combined.

DISCUSSION

To validate our experimental approach, we compared the measured *in situ* ^{14}C concentrations from the HNO_3 experiments to theoretical concentrations based on exposure of olivine in our samples to cosmic rays at the 2 calibration sites. By convention, cosmogenic nuclide production rates are referenced to sea level, high latitude (SLHL) and modern geomagnetic field intensity. The modern, SLHL production rate for *in situ* ^{14}C in quartz (SiO_2) is 18.2 ± 0.3 atoms g^{-1} yr^{-1}, which is derived from calibration site data of Pigati et al. (this volume) and assumes a spatially variable atmospheric

structure (Balco et al. 2008) and the spallogenic/muogenic production proportions of Heisinger et al. (2002). We used the spatial and temporal scaling models of Lifton et al. (2005) to account for the influence of the variations in the intensity and configuration of the Earth's magnetic field through time, solar modulation, and atmospheric depth on the secondary cosmic-ray flux. For comparison, we also used a SLHL production rate of 15.7 ± 0.2 atoms g^{-1} yr^{-1} for *in situ* ^{14}C that was calculated using the scaling model of Lal (1991), as modified by Stone (2000). For this calculation, we neglected solar and geomagnetic field effects, but included the spatially variable atmospheric structure. Based on the location and age of the basalt flows at each site, theoretical *in situ* ^{14}C concentrations for olivine at Tabernacle Hill and the McCarty's flow are (306 ± 12) and (155 ± 11) × 10^3 atoms g^{-1}, respectively, using the Lifton et al. (2005) scaling model, and (310 ± 12) and (169 ± 11) × 10^3 atoms g^{-1}, respectively, using the Lal/Stone model (Table 3).

Table 3 Measured versus theoretical *in situ* ^{14}C concentrations.[a]

	Tabernacle Hill, UT	McCarty's Flow, NM
Average measured concentration (10^3 atoms g^{-1})	108 ± 9	29 ± 4
Correction 1		
Olivine:pyroxene ratio[b]	97 : 3	63 : 37
Initial adjusted concentration (10^3 atoms g^{-1})[c]	112 ± 9	47 ± 4
Correction 2		
Fe/(Fe+Mg) ratio (in wt%)[d]	0.367 ± 0.004	0.349 ± 0.001
Final adjusted concentration (10^3 atoms g^{-1})[e]	304 ± 20	134 ± 11
Theoretical concentration (10^3 atoms g^{-1})	306 ± 12[f]	155 ± 11[f]
	310 ± 12[g]	169 ± 11[g]

[a]All uncertainties are given at the 1-σ level.
[b]Average of grain counts for randomly selected aliquots of samples from Tabernacle Hill and McCarty's flow localities (n = 20).
[c]These concentrations reflect that fact that pyroxene was not dissolved during the extraction process.
[d]Results of major element analyses are given in Appendix 1, Table A1.
[e]These concentrations assume that the proportion of *in situ* ^{14}C atoms released from the $LiBO_2$ melt was proportional to the Fe:(Fe+Mg) ratio of the olivine (see text for discussion).
[f]Calculated using the Lifton et al. (2005) scaling model.
[g]Calculated using the Lal (1991) scaling model, modified by Stone (2000).

The measured *in situ* ^{14}C concentrations for Tabernacle Hill and the McCarty's flow (Figure 4a; Table 3), (108 ± 9) and (29 ± 4) × 10^3 atoms g^{-1}, respectively, are significantly lower than these theoretical concentrations. For direct comparison, we implicitly assume that all ^{14}C atoms originally present in the olivine samples were released and ultimately collected and analyzed. Based on our results and visual inspection of the spent olivine-flux mixture in the sample boat, we do not think that this has happened for 3 reasons.

First, pyroxene and olivine are difficult to fully separate because they have similar densities and magnetic properties. For ^3He analysis, olivine grains are often hand-picked from pyroxene and matrix material, but hand-picking olivine grains for *in situ* ^{14}C measurements was not a practical option because of the large (up to 5.0 g) sample size required. Visual inspection of the spent olivine-flux mixture of our samples revealed the presence of undissolved pyroxene grains near the base of the mixture. Pyroxene grains that were not dissolved during our extractions likely did not contribute to the measured *in situ* ^{14}C concentrations. Therefore, the measured concentrations discussed above, which are given in units of atoms g^{-1}, would underestimate the *in situ* ^{14}C concentrations actually present in the samples because the denominators (sample masses) were too large. Based on grain

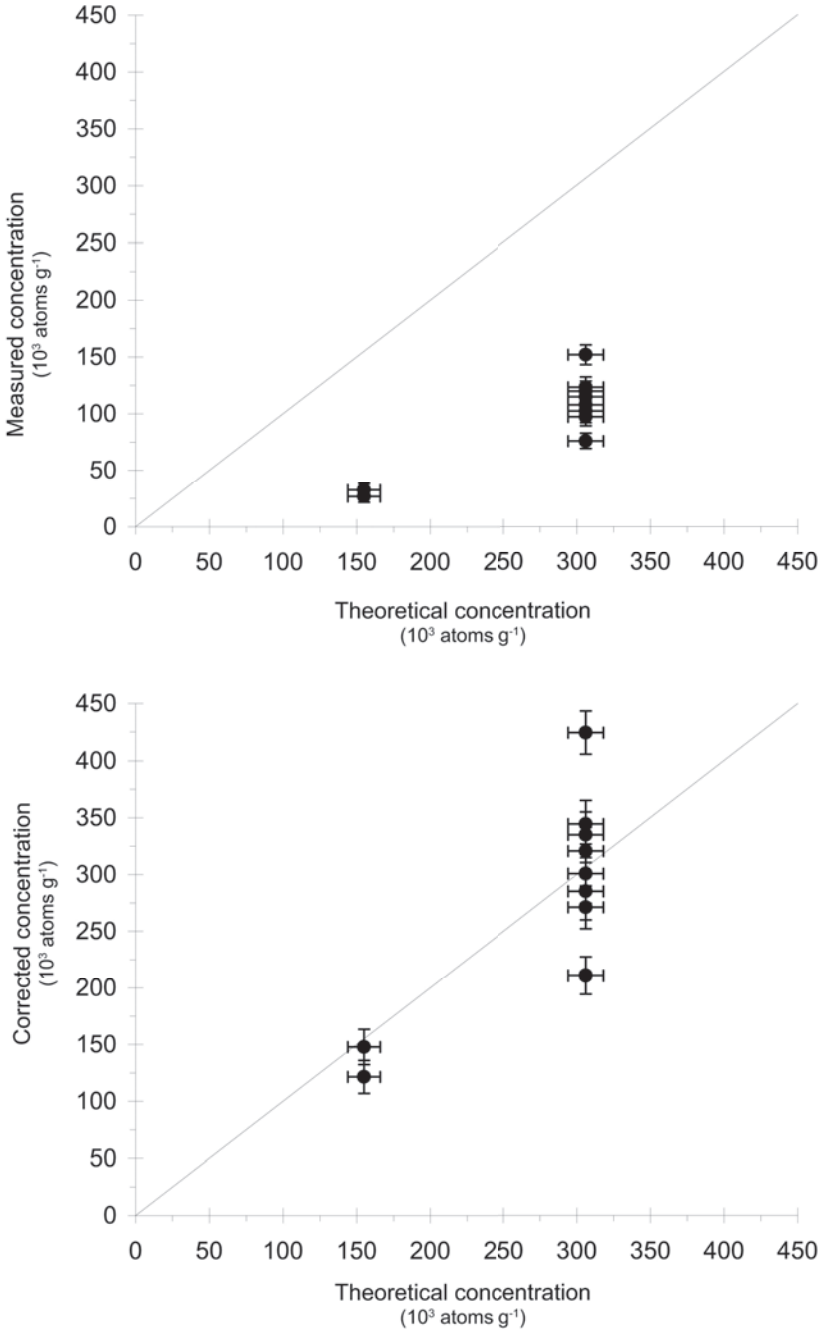

Figure 4 Theoretical *in situ* ^{14}C concentrations (calculated using Lifton et al. 2005) versus (a) measured concentrations that assume all *in situ* ^{14}C originally present in the olivine grains was released and collected, and (b) corrected *in situ* ^{14}C concentrations after empirical corrections based on the olivine:pyroxene and Fe/(Fe+Mg) ratios were applied (see text and Table 3). These corrections account for *in situ* ^{14}C atoms that were not released from the olivine-$LiBO_2$ melt. Solid diagonal lines in each frame show 1:1 values. Theoretical concentrations calculated using Lal (1991), modified by Stone (2000), are similar to those shown here.

counts of randomly selected, unprocessed subsamples, the olivine:pyroxene ratios in the Tabernacle Hill and McCarty's flow samples were approximately 97:3, and 63:37, respectively. Assuming the olivine:pyroxene mass ratio is equivalent to the grain count ratios, we can correct the measured concentrations using the grain count values. The corrected *in situ* ^{14}C concentrations for the Tabernacle Hill and McCarty's samples, (112 ± 9) and (47 ± 4) × 10^3 atoms g^{-1}, respectively, are still significantly lower than the theoretical concentrations for both sample sets (Table 3).

Second, olivine is a solid-solution series with end-members forsterite (Mg_2SiO_4) and fayalite (Fe_2SiO_4) that have very different melting points (1890 and 1205 ºC, respectively, Klein and Hurlbut 1993). For reference, quartz has a melting point of 1610 ºC (Lide 1990). Assuming that a mineral's behavior during $LiBO_2$ dissolution reflects its melting behavior (i.e. lower melting-point minerals dissolve more quickly in $LiBO_2$), Fe-crystal lattices were likely destroyed during our extraction process. However, we speculate that either the Mg-crystal lattices were not completely destroyed or there were interactions between the newly released ^{14}C and Mg atoms that prevented the release of the *in situ* ^{14}C atoms from the olivine-flux melt. In either case, we would have preferentially collected ^{14}C atoms associated with the destroyed Fe-crystal lattices and, therefore, our ^{14}C yields would have underestimated the true *in situ* ^{14}C concentration by an amount related to the proportion of Fe and Mg in our samples. Major element analysis (Table A1) showed that the average Fe/(Fe+Mg) ratios of the mineral separates were 0.367 and 0.349 for the Tabernacle Hill and McCarty's flow samples, respectively. If we use these values to correct the concentrations presented above (after the correction for undissolved pyroxene), we obtain corrected *in situ* ^{14}C concentrations of (304 ± 20) and (134 ± 11) × 10^3 atoms g^{-1} for the Tabernacle Hill and McCarty's flow samples, respectively, similar to the corresponding theoretical values (Figure 4b; Table 3).

Finally, visual inspection of the spent sample boats revealed the presence of numerous small (fine silt size) grains suspended in the solidified melt that we could not readily identify. Electron microprobe analysis revealed that the grains were synthetic spinel-like minerals composed of Al, Mg, Fe, and O. Grains located near the surface of the melt were small, angular, and composed of ~90% of Al_2O_3 with trace amounts of MgO and Fe_2O_3, whereas grains near the base of the melt were elongated, less angular, and composed of Al_2O_3 (70%), MgO (20%), and Fe_2O_3 (5%). Based on the physical and chemical characteristics of these grains, they probably formed in the $LiBO_2$ melt as a result of the interaction between the partially dissolved Al_2O_3 sample boat and the dissolved olivine grains. It is unclear exactly how these grains interacted with the *in situ* ^{14}C atoms released from olivine, if at all. It is possible that at least some of the ^{14}C atoms liberated from the olivine grains became trapped during their formation, which may account for the difference between the theoretical and corrected concentrations described above. It is also possible that the spinel-like grains may not have interacted at all with liberated *in situ* ^{14}C atoms and that a portion of the *in situ* ^{14}C atoms that were released from the olivine grains were simply retained in the melt.

Future research should include measurement of *in situ* ^{14}C concentrations in olivine from known-age basalt flows with different chemical compositions (i.e. more Fe-rich) to determine if our series of corrections to the measured *in situ* ^{14}C concentrations are robust for all olivine-bearing rocks. If so, then researchers could potentially use *in situ* ^{14}C for cosmogenic research in terrain with olivine-bearing rocks, but should do so now only if cognizant of the uncertainties and limitations of the process as it stands today.

CONCLUSIONS

The experimental data presented here summarizes a series of chemical pretreatment and step-heating experiments aimed at extracting *in situ* ^{14}C from olivine. After experimenting with a number of combinations of acids, acid strength, and duration of acid treatments, we were able to extract a stable and reproducible *in situ* ^{14}C component from olivine following treatment with dilute HNO_3 over a variety of experimental conditions. However, the measured *in situ* ^{14}C concentrations in olivine from 2 calibration sites, the Tabernacle Hill and McCarty's basalt flows, were significantly lower than theoretical values based on exposure of olivine to cosmic rays at these sites. The source of the discrepancy is not clear. We speculate that *in situ* ^{14}C atoms may not have been released from Mg-rich crystal lattices during the heating process (the olivine composition at both sites was ~$Fo_{65}Fa_{35}$). Alternatively, a portion of the ^{14}C atoms released from the olivine grains may have become trapped in synthetic spinel-like minerals that were created in the olivine-flux mixture during the extraction process, or were simply retained in the mixture itself. Regardless, the magnitude of the discrepancy appears to be inversely proportional to the Fe/(Fe+Mg) ratio of the olivine separates. If we apply a simple correction factor based on the chemical composition of the separates, then corrected *in situ* ^{14}C concentrations are similar to theoretical values at both sites. At this time, we do not know if this agreement is fortuitous, limited to olivines with ~$Fo_{65}Fa_{35}$ compositions, or robust. Future research should include measurement of *in situ* ^{14}C concentrations in olivine from known-age basalt flows with different chemical compositions (i.e. more Fe-rich) to determine if this correction is applicable to all olivine-bearing rocks.

ACKNOWLEDGMENTS

We thank Herschel Schultz at the El Malpais National Monument for sampling permission and Ken Domanik at the University of Arizona for laboratory assistance and analysis of our electron microprobe data. We thank Rich Cruz and the Arizona AMS facility for their support. Early versions of this manuscript benefited from constructive reviews from G Cook, J Schaefer, and an anonymous reviewer. The current version of this manuscript was improved by careful reviews by E Ellis, G Landis, J Paces, Y Yokoyama, and an anonymous reviewer.

REFERENCES

Balco G, Stone JO, Lifton NA, Dunai TJ. 2008. A complete and easily accessible means of calculating surface exposure ages or erosion rates from ^{10}Be and ^{26}Al measurements. *Quaternary Geochronology* 3(3):174–95.

Benson LV. 1978. Fluctuation in the level of pluvial Lake Lahontan during the last 40,000 years. *Quaternary Research* 9(3):300–18.

Bevington PR, Robinson DK. 1992. *Data Reduction and Error Analysis for the Physical Sciences*. Boston: McGraw-Hill. 328 p.

Blard P-H, Bourlès D, Pik R, Lavé J. 2008. In situ cosmogenic ^{10}Be in olivines and pyroxenes. *Quaternary Geochronology* 3(3):196–205.

Broecker WS, Kaufman A. 1965. Radiocarbon chronology of Lake Lahontan and Lake Bonneville II, Great Basin. *Geological Society of America Bulletin* 76(5): 537–66.

Cerling TE. 1990. Dating geomorphologic surfaces using cosmogenic ^{3}He. *Quaternary Research* 33(2): 148–56.

Godsey HS, Currey DR, Chan MA. 2005. New evidence for an extended occupation of the Provo shoreline and implications for regional climate change, Pleistocene Lake Bonneville, Utah, USA. *Quaternary Research* 63(2):212–23.

Gordon MS, Goldhagen P, Rodbell KP, Zabel TH, Tang HK, Clem JM, Bailey P. 2004. Measurement of the flux and energy spectrum of cosmic-ray induced neutrons on the ground. *IEEE Transactions on Nuclear Science* 51(6):3427–334.

Gosse JC, Phillips FM. 2001. Terrestrial in situ cosmogenic nuclides: theory and application. *Quaternary Science Reviews* 20(14):1475–560.

Handwerger DA, Cerling TE, Bruhn RL. 1999. Cosmogenic ^{14}C in carbonate rocks. *Geomorphology* 27(1–2):13–24.

Heisinger B, Lal D, Jull AJT, Kubik P, Ivy-Ochs S, Neumaier S, Knie K, Lazarev V, Nolte E. 2002. Production of selected cosmogenic radionuclides by muons: 1. Fast muons. *Earth and Planetary Science Letters* 200(3–4):345–55.

Hippe K, Kober F, Baur H, Ruff M, Wacker L, Wieler R. 2009. The current performance of the *in situ* ^{14}C extraction line at ETH. *Quaternary Geochronology* 4(6): 493–500.

Kamilli RJ, Richard SM. 1998. *Geologic Highway Map of Arizona*. Tucson: Arizona Geological Society and Arizona Geological Survey.

Klein C, Hurlbut CS. 1993. *Manual of Mineralogy.* New York: John Wiley & Sons, Inc. 681 p.

Kohl CP, Nishiizumi K. 1992. Chemical isolation of quartz for measurement of *in-situ*-produced cosmogenic nuclides. *Geochimica et Cosmochimica Acta* 56(9):3583–7.

Lal D. 1988. In situ-produced cosmogenic isotopes in terrestrial rocks. *Annual Reviews of Earth and Planetary Sciences* 16:355–88.

Lal D. 1991. Cosmic ray labeling of erosion surfaces: *in situ* nuclide production rates and erosion models. *Earth and Planetary Science Letters* 104(2–4):424–39.

Laughlin AW, Poths J, Healey HA, Reneau S, Wolde-Gabriel G. 1994. Dating of Quaternary basalts using the cosmogenic ^{3}He and ^{14}C methods with implications for excess ^{40}Ar. *Geology* 22(2):135–8.

Lide DR, editor-in-chief. 1990. *CRC Handbook of Chemistry and Physics*. 78th edition. Boca Raton: CRC Press. 2512 p.

Lifton NA, Jull AJT, Quade J. 2001. A new extraction technique and production rate estimate for *in situ* cosmogenic ^{14}C in quartz. *Geochimica et Cosmochimica Acta* 65(12):1953–69.

Lifton NA, Bieber JW, Clem JM, Duldig ML, Evenson P, Humble JE, Pyle R. 2005. Addressing solar modulation and long-term uncertainties in scaling in situ cosmogenic nuclide production rates. *Earth and Planetary Science Letters* 239(1–2):140–61.

Marti K, Craig H. 1987. Cosmic-ray-produced neon and helium in the summit lavas of Maui. *Nature* 325(6102):335–7.

Miller GH, Briner JB, Lifton NA, Finkel RC. 2006. Limited ice-sheet erosion and complex exposure histories derived from in situ cosmogenic ^{10}Be, ^{26}Al, and ^{14}C on Baffin Island, Arctic Canada. *Quaternary Geochronology* 1(1):74–85.

Naysmith P. 2007. Extraction and measurement of cosmogenic *in situ* ^{14}C from quartz [unpublished manuscript]. University of Glasgow. 94 p.

Nieminen M, Torsti JJ, Valtonen E, Arvela H, Lumme M, Peltonen J, Vainikka E. 1985. Composition and spectra of cosmic-ray hadrons at sea level. *Journal of Physics G Nuclear and Particle Physics* 11:421–37.

Nishiizumi K, Klein J, Middleton R, Craig H. 1990. Cosmogenic ^{10}Be, ^{26}Al, and ^{3}He in olivine from Maui lavas. *Earth and Planetary Science Letters* 98(3–4): 263–6.

Oviatt CG, Nash WP. 1989. Late Pleistocene basaltic ash and volcanic eruptions in the Bonneville basin, Utah. *Geological Society of America Bulletin* 101(2):292–303.

Oviatt CG, Currey DR, Sack D. 1992. Radiocarbon chronology of Lake Bonneville, Eastern Great Basin, USA. *Palaeogeography, Palaeoclimatology, Palaeoecology* 99(3–4):225–41.

Phillips FM, Zreda MG, Flinsch MR, Elmore D, Sharma P. 1996. A reevaluation of cosmogenic ^{36}Cl production rates in terrestrial rocks. *Geophysical Research Letters* 23(9):949–52.

Pigati JS, Lifton NA, Jull AJT, Quade J. 2010. A simplified *in situ* cosmogenic ^{14}C extraction system. *Radiocarbon* 52(2–3):1236–43.

Poreda RJ, Cerling TE. 1992. Cosmogenic neon in recent lavas from the western United States. *Geophysical Research Letters* 19(18):1863–6.

Reimer PJ, Baillie MGL, Bard E, Bayliss A, Beck JW, Bertrand CJH, Blackwell PG, Buck CE, Burr GS, Cutler KB, Damon PE, Edwards RL, Fairbanks RG, Friedrich M, Guilderson TP, Hogg AG, Hughen KA, Kromer B, McCormac G, Manning S, Bronk Ramsey C, Reimer RW, Remmele S, Southon JR, Stuiver M, Talamo S, Taylor FW, van der Plicht J, Weyhenmeyer CE. 2004. IntCal04 terrestrial radiocarbon age calibration, 0–26 cal kyr BP. *Radiocarbon* 46(3):1029–58.

Shimaoka A, Kong P, Finkel RC, Caffee MW, Nishiizumi K. 2002. The determination of *in situ* radionuclides in olivine [abstract]. 12th annual V.M. Goldschmidt Conference. *Geochimica et Cosmochimica Acta*. Davos, Switzerland. p 709.

Slota Jr PJ, Jull AJT, Linick TW, Toolin LJ. 1987. Preparation of small samples for ^{14}C accelerator targets by catalytic reduction of CO. *Radiocarbon* 29(2):303–6.

Stone JO. 2000. Air pressure and cosmogenic isotope production. *Journal of Geophysical Research* 105(B10):23,753–9.

Stuiver M, Reimer PJ. 1993. Extended ^{14}C data base and revised CALIB 3.0 ^{14}C age calibration program. *Radiocarbon* 35(1):215–30.

Trull TW, Kurz MD, Jenkins WJ. 1991. Diffusion of cosmogenic He-3 in olivine and quartz: implications for surface exposure dating. *Earth and Planetary Science Letters* 103(1–4):241–6.

Yokoyama Y, Caffee MW, Southon JR, Nishiizumi K. 2004. Measurements of *in situ* produced ^{14}C in terrestrial rocks. *Nuclear Instruments and Methods in Physics Research B* 223–224:253–8.

Zreda MG, Phillips FM, Elmore D, Kubik PW, Sharma P, Dorn RI. 1991. Cosmogenic chlorine-36 production rates in terrestrial rocks. *Earth and Planetary Science Letters* 105(1–3):94–109.

APPENDIX 1

Table A1 Analytical results.

Sample ID	Lab ID	SiO_2 %	Al_2O_3 %	Fe_2O_3 %	MnO %	MgO %	CaO %	Na_2O %	K_2O %	TiO_2 %	P_2O_5 %
PP-4 (quartz)[a]	RN-758	98.28	0.86	0.29	0.00	0.31	0.03	0.07	0.07	0.08	0.00
TH-15	RN-741	42.82	1.27	20.04	0.26	34.54	0.75	0.18	0.00	0.11	0.03
TH-15	RN-745	42.63	1.60	20.45	0.26	33.83	0.76	0.22	0.10	0.13	0.02
TH-15	RN-751	42.95	1.66	19.58	0.26	34.15	0.90	0.26	0.04	0.14	0.05
TH-15	RN-754	43.73	2.63	18.71	0.25	32.59	1.04	0.63	0.18	0.18	0.05
McC-1b	RN-771	40.25	2.87	18.77	0.22	34.99	1.88	0.52	0.13	0.30	0.06
AZ02-2	RN-749	43.14	2.43	22.85	0.38	27.88	2.61	0.43	0.09	0.17	0.02

[a]See Pigati et al. (this volume) for sample details.

Table A2 Summary of data for individual temperature steps for all experiments.[a]

Lab #	AMS #	Sample ID	Fraction modern[b]	Sample volume (μL)	Diluted volume (mL)[c]	^{14}C yield (10^3 atoms g^{-1})[d]
Abbreviations in Equation 1			F_m	V_s	V_s	N
HF experiments						
RN-725a	53333	TH-1-olivine-300	0.0047 ± 0.0004	9.48 ± 1.06	1.23 ± 0.01	35 ± 6
RN-725b	53333	TH-1-olivine-500	0.0023 ± 0.0004	6.70 ± 1.14	1.14 ± 0.01	8 ± 5
RN-725c	53333	TH-1-olivine-600	0.0003 ± 0.0003	3.01 ± 0.98	1.21 ± 0.01	0 ± 4
RN-725d	53333	TH-1-olivine-700	–0.0004 ± 0.0002	1.15 ± 1.22	1.14 ± 0.01	0 ± 3
RN-725e	53333	TH-1-olivine-900	0.0000 ± 0.0003	0.93 ± 1.02	1.19 ± 0.01	0 ± 3
RN-725f	53333	TH-1-olivine-1100-1st hr	0.0075 ± 0.0003	3.92 ± 1.22	1.19 ± 0.01	61 ± 4
RN-725g	53333	TH-1-olivine-1100-2nd hr	0.0002 ± 0.0004	8.55 ± 1.14	1.16 ± 0.01	0 ± 5
RN-725h	53333	TH-1-olivine-1100-3rd hr	0.0027 ± 0.0003	3.69 ± 1.22	1.16 ± 0.01	1 ± 4
RN-728a	53333	TH-1-olivine-300	0.0044 ± 0.0003	6.93 ± 1.14	1.31 ± 0.01	35 ± 5
RN-728b	53333	TH-1-olivine-500	0.0073 ± 0.0006	15.94 ± 1.15	1.30 ± 0.01	60 ± 8
RN-728c	53333	TH-1-olivine-600	0.0023 ± 0.0003	1.84 ± 1.22	1.23 ± 0.01	21 ± 3
RN-728d	53333	TH-1-olivine-700	0.0015 ± 0.0003	1.16 ± 1.10	1.28 ± 0.01	14 ± 4
RN-728e	53333	TH-1-olivine-900	0.0014 ± 0.0004	3.71 ± 0.98	1.24 ± 0.01	8 ± 4
RN-728f	53333	TH-1-olivine-1100-1st hr	0.0077 ± 0.0003	8.55 ± 1.10	1.26 ± 0.01	49 ± 5
RN-728g	53333	TH-1-olivine-1100-2nd hr	0.0049 ± 0.0006	3.45 ± 1.30	1.22 ± 0.01	23 ± 6
RN-728h	53333	TH-1-olivine-1100-3rd hr	0.0018 ± 0.0003	1.85 ± 1.14	1.21 ± 0.01	11 ± 5
RN-739a	55357	TH-13-olivine-300	0.0147 ± 0.0005	24.92 ± 1.19	1.39 ± 0.01	145 ± 13
RN-739b	55357	TH-13-olivine-500	0.0197 ± 0.0005	37.12 ± 1.23	1.35 ± 0.01	187 ± 16
RN-739c	55357	TH-13-olivine-600	0.0145 ± 0.0006	17.35 ± 1.07	1.29 ± 0.01	139 ± 13
RN-739d	55357	TH-13-olivine-700	0.0095 ± 0.0004	16.34 ± 1.30	1.34 ± 0.01	95 ± 9
RN-739e	55357	TH-13-olivine-900	0.0082 ± 0.0004	13.65 ± 1.07	1.32 ± 0.01	75 ± 7
RN-739f	55357	TH-13-olivine-1100-1st hr	0.0143 ± 0.0003	17.10 ± 1.11	1.31 ± 0.01	115 ± 10
RN-739g	55357	TH-13-olivine-1100-2nd hr	0.0058 ± 0.0004	4.17 ± 1.02	1.26 ± 0.01	33 ± 5
RN-739h	55357	TH-13-olivine-1100-3rd hr	0.0035 ± 0.0003	2.08 ± 1.06	1.16 ± 0.01	26 ± 5
HCl experiments						
RN-721a	55357	TH-13-olivine-300	0.0162 ± 0.0006	30.90 ± 1.23	1.52 ± 0.01	182 ± 13
RN-721b	55357	TH-13-olivine-400	0.0176 ± 0.0005	32.97 ± 1.23	1.42 ± 0.01	167 ± 12
RN-721c	55357	TH-13-olivine-500	0.0122 ± 0.0004	24.48 ± 1.15	1.45 ± 0.01	132 ± 9
RN-721d	55357	TH-13-olivine-600	0.0142 ± 0.0013	26.05 ± 1.23	1.53 ± 0.01	161 ± 18
RN-721e	55357	TH-13-olivine-700	0.0139 ± 0.0005	30.41 ± 1.27	1.47 ± 0.01	146 ± 10
RN-721f	55357	TH-13-olivine-900	0.0165 ± 0.0006	28.13 ± 1.23	1.49 ± 0.01	178 ± 12
RN-721g	55357	TH-13-olivine-1100-1st hr	0.0054 ± 0.0003	7.61 ± 1.22	1.46 ± 0.01	36 ± 5
RN-721h	55357	TH-13-olivine-1100-2nd hr	0.0025 ± 0.0003	1.84 ± 1.22	1.41 ± 0.01	10 ± 4

Table A2 Summary of data for individual temperature steps for all experiments.[a] *(Continued)*

Lab #	AMS #	Sample ID	Fraction modern[b]	Sample volume (μL)	Diluted volume (mL)[c]	^{14}C yield (10^3 atoms g^{-1})[d]
RN-721i	55357	TH-13-olivine-1100-3rd hr	0.0006 ± 0.0004	1.61 ± 1.22	1.38 ± 0.01	1 ± 5
RN-730a	55357	TH-13-olivine-300	0.0313 ± 0.0006	35.48 ± 1.27	1.22 ± 0.01	275 ± 22
RN-730b	55357	TH-13-olivine-500	0.0563 ± 0.0007	82.70 ± 1.32	1.26 ± 0.01	513 ± 40
RN-730c	55357	TH-13-olivine-600	0.0182 ± 0.0004	9.90 ± 1.30	1.13 ± 0.01	152 ± 13
RN-730d	55357	TH-13-olivine-700	0.0164 ± 0.0004	3.92 ± 1.26	1.17 ± 0.01	141 ± 12
RN-730e	55357	TH-13-olivine-900	0.0145 ± 0.0006	6.22 ± 1.26	1.14 ± 0.01	117 ± 11
RN-730f	55357	TH-13-olivine-1100-1st hr	0.0226 ± 0.0005	10.14 ± 1.26	1.16 ± 0.01	170 ± 14
RN-730g	55357	TH-13-olivine-1100-2nd hr	0.0116 ± 0.0004	2.54 ± 1.22	1.12 ± 0.01	74 ± 7
RN-730h	55357	TH-13-olivine-1100-3rd hr	0.0047 ± 0.0004	1.38 ± 1.18	1.64 ± 0.01	53 ± 8
RN-736a	55357	TH-13-olivine-300	0.0327 ± 0.0005	53.54 ± 1.21	1.67 ± 0.01	399 ± 32
RN-736b	55357	TH-13-olivine-500	0.0405 ± 0.0007	78.16 ± 1.27	1.68 ± 0.01	495 ± 39
RN-736c	55357	TH-13-olivine-600	0.0173 ± 0.0009	14.78 ± 1.15	1.55 ± 0.01	199 ± 19
RN-736d	55357	TH-13-olivine-700	0.0210 ± 0.0003	13.60 ± 1.22	1.60 ± 0.01	250 ± 20
RN-736e	55357	TH-13-olivine-900	0.0261 ± 0.0013	17.29 ± 1.23	1.58 ± 0.01	301 ± 28
RN-736f	55357	TH-13-olivine-1100-1st hr	0.0119 ± 0.0004	11.99 ± 1.22	1.57 ± 0.01	114 ± 11
RN-736g	55357	TH-13-olivine-1100-2nd hr	0.0149 ± 0.0007	2.31 ± 1.14	1.52 ± 0.01	146 ± 14
RN-736h	55357	TH-13-olivine-1100-3rd hr	0.0010 ± 0.0003	2.55 ± 1.02	1.51 ± 0.01	7 ± 5
HNO_3 experiments						
RN-741a	55359	TH-15-olivine-300	0.0127 ± 0.0004	22.63 ± 0.67	1.35 ± 0.01	118 ± 9
RN-741b	55359	TH-15-olivine-500	0.0242 ± 0.0008	38.03 ± 0.68	1.11 ± 0.00	186 ± 13
RN-741c	55359	TH-15-olivine-600	0.0010 ± 0.0003	3.50 ± 0.66	1.20 ± 0.01	9 ± 3
RN-741d	55359	TH-15-olivine-700	0.0004 ± 0.0002	2.57 ± 0.66	1.17 ± 0.01	3 ± 3
RN-741e	55359	TH-15-olivine-900	0.0009 ± 0.0002	7.05 ± 0.33	2.20 ± 0.01	9 ± 3
RN-741f	55359	TH-15-olivine-1100-1st hr	0.0125 ± 0.0004	13.67 ± 0.99	1.18 ± 0.01	84 ± 7
RN-741g	55359	TH-15-olivine-1100-2nd hr	0.0015 ± 0.0003	3.03 ± 0.74	1.64 ± 0.01	0 ± 4
RN-741h	55359	TH-15-olivine-1100-3rd hr	0.0011 ± 0.0003	2.10 ± 0.62	1.80 ± 0.01	10 ± 6
RN-745a	55359	TH-15-olivine-300	0.0160 ± 0.0004	24.14 ± 0.11	1.49 ± 0.01	173 ± 12
RN-745b	55359	TH-15-olivine-500	0.0256 ± 0.0005	42.18 ± 0.25	1.48 ± 0.01	276 ± 17
RN-745c	55359	TH-15-olivine-600	0.0028 ± 0.0003	3.28 ± 0.46	1.40 ± 0.01	29 ± 4
RN-745d	55359	TH-15-olivine-700	0.0034 ± 0.0003	2.35 ± 0.37	1.36 ± 0.01	35 ± 5
RN-745e	55359	TH-15-olivine-900	0.0039 ± 0.0003	7.07 ± 0.17	1.35 ± 0.01	34 ± 4
RN-745f	55359	TH-15-olivine-1100-1st hr	0.0142 ± 0.0004	12.19 ± 0.42	1.28 ± 0.01	113 ± 8
RN-745g	55359	TH-15-olivine-1100-2nd hr	0.0046 ± 0.0004	1.89 ± 0.17	1.28 ± 0.01	23 ± 5
RN-745h	55359	TH-15-olivine-1100-3rd hr	0.0025 ± 0.0003	1.89 ± 0.17	1.26 ± 0.01	19 ± 5
RN-751a	55359	TH-15-olivine-300	0.0089 ± 0.0003	18.25 ± 1.15	1.67 ± 0.01	102 ± 7
RN-751b	55359	TH-15-olivine-500	0.0199 ± 0.0004	47.42 ± 1.32	1.68 ± 0.01	236 ± 15
RN-751c	55359	TH-15-olivine-600	0.0013 ± 0.0002	4.63 ± 1.02	1.63 ± 0.01	15 ± 3
RN-751d	55359	TH-15-olivine-700	0.0011 ± 0.0002	2.31 ± 1.14	1.61 ± 0.01	12 ± 3
RN-751e	55359	TH-15-olivine-900	0.0010 ± 0.0002	5.53 ± 1.22	1.59 ± 0.01	6 ± 3
RN-751f	55359	TH-15-olivine-1100-1st hr	0.0091 ± 0.0003	14.97 ± 1.26	1.58 ± 0.01	82 ± 7
RN-751g	55359	TH-15-olivine-1100-2nd hr	0.0017 ± 0.0003	2.76 ± 1.26	1.55 ± 0.01	0 ± 4
RN-751h	55359	TH-15-olivine-1100-3rd hr	0.0005 ± 0.0003	1.61 ± 1.30	1.54 ± 0.01	1 ± 5
RN-754a	55359	TH-15-olivine-600	0.0044 ± 0.0003	4.19 ± 0.82	1.28 ± 0.01	45 ± 6
RN-754b	55359	TH-15-olivine-1100 (3 hr)	0.0150 ± 0.0004	32.32 ± 0.83	1.45 ± 0.01	114 ± 9
RN-756a	55359	TH-15-olivine-600	0.0033 ± 0.0003	1.86 ± 0.74	1.38 ± 0.01	34 ± 5
RN-756b	55359	TH-15-olivine-1100 (3 hr)	0.0167 ± 0.0004	23.48 ± 0.83	1.41 ± 0.01	123 ± 9
RN-774a	55359	TH-15-olivine-600	0.0041 ± 0.0003	2.09 ± 0.90	1.10 ± 0.00	33 ± 5
RN-774b	55359	TH-15-olivine-1100 (3 hr)	0.0161 ± 0.0005	18.77 ± 0.99	1.10 ± 0.01	75 ± 7
RN-776a	55359	TH-15-olivine-600	0.0060 ± 0.0003	3.70 ± 1.14	1.07 ± 0.00	47 ± 6
RN-776b	55359	TH-15-olivine-1100 (3 hr)	0.0192 ± 0.0006	23.87 ± 0.99	1.08 ± 0.00	97 ± 8
RN-777a	55359	TH-15-olivine-700	0.0044 ± 0.0003	3.24 ± 1.06	1.05 ± 0.00	34 ± 4
RN-777b	55359	TH-15-olivine-800	0.0025 ± 0.0003	1.85 ± 1.14	1.04 ± 0.00	17 ± 4
RN-777c	55359	TH-15-olivine-900	0.0032 ± 0.0003	3.00 ± 1.14	1.03 ± 0.00	19 ± 3

Table A2 Summary of data for individual temperature steps for all experiments.[a] *(Continued)*

Lab #	AMS #	Sample ID	Fraction modern[b]	Sample volume (μL)	Diluted volume (mL)[c]	^{14}C yield (10^3 atoms g^{-1})[d]
RN-777d	55359	TH-15-olivine-1100 (3 hr)	0.0181 ± 0.0004	15.05 ± 1.03	1.03 ± 0.00	81 ± 6
RN-779[e]	55356	TH-12-olivine-1100 (3 hr)	0.0238 ± 0.0005	24.18 ± 0.83	0.99 ± 0.00	119 ± 9
RN-771a	60994	McC-1b-600	0.0004 ± 0.0003	1.85 ± 1.14	1.13 ± 0.01	3 ± 5
RN-771b	60994	McC-1b-1100(3)	0.0097 ± 0.0003	22.65 ± 1.11	1.14 ± 0.01	27 ± 5
RN-772[e]	60994	McC-1b-1100 (3 hr)	0.0104 ± 0.0003	25.49 ± 0.99	1.13 ± 0.01	32 ± 6

[a]All uncertainties are given at the 1-σ level.

[b]Fraction modern values are referenced to the NIST oxalic acid I standard (Stuiver and Polach 1977).

[c]CO_2 extracted from each sample was diluted with ^{14}C-free CO_2 before conversion to graphite.

[d]*In situ* ^{14}C yields for all samples were normalized to production at the ground surface, open-sky conditions (no topographic shielding), and a pure SiO_2 composition using the correction factors listed in Table 1. All values are corrected using blanks listed in Table 2 of Pigati et al. (this volume).

[e]*In situ* ^{14}C yields for RN-772 and -779 include ^{14}C atoms recovered at 600 ºC.